THE EUROPEAN
PHYSICAL JOURNAL PLUS

Non-destructive exploration of late Gothic panel painting using X-ray tomography and flattening of the reconstructed data

Daniel Vavřík[1,a] , **Václava Antušková**[2], **Štěpánka Chlumská**[2], **Ivana Kumpová**[1], **Radka Šefců**[2], **Michal Vopálenský**[1]

[1] Institute of Theoretical and Applied Mechanics, Czech Academy of Sciences, Prosecká 76, Prague 9, Czech Republic
[2] National Gallery Prague, Staroměstské nám. 12, 110 15 Prague 1, Czech Republic

Abstract The use of computed tomography (CT) for studying artwork has a long tradition in the restoration and care of collections in memory institutions. The result of the related tomographic reconstruction is a virtual spatial model in which we can examine the production technology, the internal structure, various damaged areas, and previous restoration interventions. The extension of standard CT to dual energy CT provides additional information to help distinguish materials with similar densities but different chemical compositions. As will be shown, pigment differences that appear very similar in optical light can be identified in this way. The differences found were confirmed by X-ray fluorescence and Raman spectroscopy analytical techniques. Current laboratory CT scanners make it possible to examine the layered structures of paintings and polychrome sculptures. In the case of wood panel paintings, however, we are faced with the common deformation of the panels. So, when examining the CT data, we can only see a small section of the paint layer, and it is difficult to examine the whole artwork in its entire context. This disadvantage can be solved by a virtual straightening of the panel, as will be demonstrated.

1 Introduction

The presented results were obtained by an interdisciplinary survey of a medieval Bohemian panel painting, Virgin and Child on a Crescent Moon from the Collection of Vojtěch Lanna [1–3] (South Bohemia, ca 1450, inv. no O 495, 41.5 × 31.5 cm), from the collection of the National Gallery Prague (NGP). The central theme of the painting is the Virgin Mary supplemented by paintings of saints and donors on the frame, See Fig. 1a, and for a backside imitation of a stone slab, see Fig. 1b.

The profiled board, made from one piece of wood, serves as a support of the painting. On the top and bottom edges, the board is reinforced with inset slabs visible on the reverse side, see Fig. 1b. The original painting covers the central panel, the frame, and even the backside. Therefore, we only have a limited possibility to document the condition of the wood panel by means of common optical methods. The documentation of the wooden inner structure is essential, for example, for obtaining data on a dendrochronological analysis [4]. For this reason, the painting was chosen for tomographic investigation, which was performed at the Institute of Theoretical and Applied Mechanics, Centre Telč [5]. Restoration and material research at the Department of Conservation and the Restoration and Chemical-Technological Laboratory of the National Gallery Prague preceded this investigation. The obtained results were compared with an older restoration report by Radim Klouza from year 2000, stored at the Archive of the Department of Conservation and Restoration. The restoration research included photographic documentation in different light modes (incident daylight, raking light, UV luminescence), IR reflectography, and X-ray documentation.[1]

With respect to the small dimensions and condition of the painting, material research was conducted in an exclusively in a non-invasive way. Photomicrographic documentation of the surface, structural analysis via Raman spectroscopy, and elemental analysis by means of X-ray fluorescence analysis were performed to get information about the pigments used. The main disadvantage of non-invasive methods is that we usually obtain summary results from several layers. Therefore, we cannot identify the stratigraphy (the system of layering) and the composition of individual layers. Also, using these methods, it is not possible to identify binders.

X-ray Computed Tomography and Dual Energy Computed Tomography, in conjunction with post-processing of the tomographic data, were used to obtain further information about the structure of the wood panel and its manufacturing technology. Furthermore, the stratigraphy of the paint layer was analysed on the basis of tomographic reconstructed data using especially in-house developed software.

---

[1] The restoration research in 2022 was conducted by Adam Pokorný, Department of Conservation and Restoration of the National Gallery in Prague, whom we would like to thank.

---

a e-mail: vavrik@itam.cas.cz (corresponding author)

Fig. 1 Painting Virgin and Child on a Crescent Moon, obverse, and reverse

2 X-ray computed tomography for artwork investigation

X-ray computed tomography (CT) is a non-invasive technique that provides information about the internal morphology of the object under examination. Using CT, a complete 3D reconstruction of the object under analysis is possible, overcoming an important limitation of radiography, i.e. the overlapping of features belonging to different layers of the object in the image. The CT technique is also currently used for various cultural heritage objects, including wooden paintings, where, like in this work, a combination with other techniques related to the identification of pigments and preparatory materials has been published [6, 7]. It has also been shown that the CT technique can be used to date panel paintings based on dendrochronology [8]. It should be emphasised that CT resolution plays a crucial role in the detailed study of artifacts. Depending on the design of the CT scanner (tomograph) and the size of the object, the CT resolution of wooden paintings can range from tenths [8] to hundreds of micrometres [9].

For this study, the computed tomography laboratory, located in the Centre Telč (CET) of the Institute of Theoretical and Applied Mechanics, was employed. This CT laboratory is equipped with a research dual-source tomograph that allows the examination of various objects with wide variability of the scanning geometry [10]. The actual resolution achievable depends on the dimensions of the object under examination and the imaging detector used. Micrometric features can be resolved on one side for objects a few millimetres in size, and a resolutions better than 200 μm for artworks hundreds of millimetres in size are available.

Thousands of X-ray images (projections) must be recorded as input data for the CT reconstruction, which are taken whilst the object is rotated relative to the X-ray detector. Based on these projections, a three-dimensional virtual model of the internal structure of the object is created. The tomographic model itself consists of a three-dimensional matrix (volume) of voxels (volume pixels) whose values represent the density of the object at a given location. CT density includes both the homogeneity (i.e. whether only one material is present in a particular voxel and/or whether there is any porosity) of the material and its chemical composition. The resolution of both possible causes of CT density can be done by Dual Energy Computed Tomography (DECT), which is based on CT measurements taken at two different X-ray spectra. The two subsequently reconstructed volumes are then linearly combined with a specific weighting factor, where its appropriately chosen value allows highlighting the selected material components [11].

The tomographically created volume is usually analysed in detail by displaying its planar sections. If the density of the material is lower at a given location, this location will be darker in the section and vice versa. If the object being analysed is not planar, the features under investigation may be only partially visible in the selected section. In this case, it is necessary to evaluate several adjacent sections to get a complete picture of the feature under investigation. Significant deformations of the panel can be encountered in wooden panel paintings. In such cases, however, the reconstructed image can be "flattened" using special software, as will be shown in the chapter "Flattening of the tomographic volume".

3 Virgin and child on a crescent moon survey based on standard and dual energy CT

When researching artworks from the NGP collection, special care was needed to ensure maximum protection of the examined artworks and to standardise the procedures for mounting them in the tomographic apparatus. The painting, packed in non-woven fabric Tyvek (by DuPont), was placed in a wooden box without any metal joints. It ensured the separation of the artwork from the

Fig. 2 Rendering of the object surface **a** the panel manufacturing technology can be seen in the 3D visualisation **b** where the reconstructed volume has been cropped from the back to show the internal structure
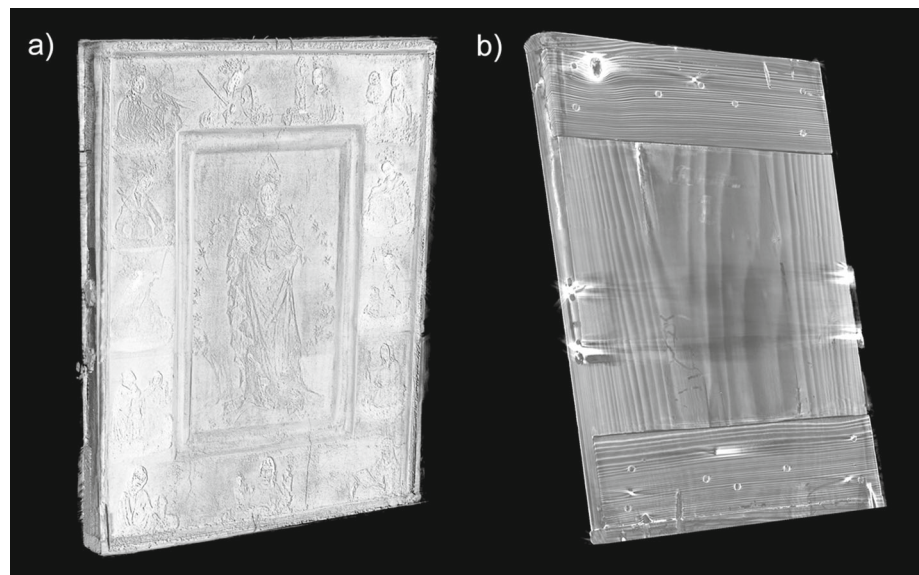
box in the resulting tomographic volume. The fabric has a lower attenuation of X-rays than the object under examination, which serves to minimise its effect on the quality of the tomography.

During one CT measurement, 2880 one-second projections were recorded on the fly (without stopping the rotation stage) to reduce measurement time. Due to the height of the image, it was necessary to record tomographic data in two different vertical positions; the resulting reconstructed volumes were then stitched together. The artwork was examined using two different acceleration voltages of 80 kV and 180 kV, where the filtering of the X-ray beam by a 0.9 mm thick brass filter at the higher voltage was used to suppress the lower part of the X-ray spectrum. This resulted in a total of four tomographic measurements. A flat panel detector (XRD-1622-AP-14, Perkin Elmer, DE) with an active area of 400×400 mm and 2048×2048 pixels with a pixel pitch of 200 µm was used. The geometric magnification was set to $1.2 \times$ by selecting the distances between the X-ray tube, the rotary table, and the imaging detector, resulting in an imaging pixel pitch of 167 µm.

CT reconstruction using a filtered back projection was performed using VGmax software (Volume Graphics, Germany). The resolution was resampled two times perpendicular to the panel painting to improve the stratigraphic resolution, i.e. the resulting voxels have $167.4 \times 167.4 \times 83.7$ µm.

An overview image of the front outer surface of the tomographically created volume is shown in Fig. 2a. Looking inside this virtual model, we can see that the panel was made from a single piece of wood, with mouldings on the top and bottom edges, and the panel is reinforced on the back side with crossbars, see Fig. 2b. In the same picture, the holes made by wood-boring insects are clearly visible. The image data from the tomographic panel model were also provided for dendrochronological analysis. Unfortunately, although it was verified that the data quality was very good for such a study, dendrochronological dating was not possible due to the insufficient number (23) of wood rings identified.

The battens and planks are glued to the panel and secured with wooden pegs. In some places, the joints between these parts are broken, see Fig. 3. It is possible to distinguish the glue layer and the preparation of the surfaces for gluing, Fig. 3a. Looking at the wooden structure and the calculated density, three different types of wood can be recognised.

Figure 4a shows a section parallel to the plane of the panel, close to the front surface. The painting on the frame is partially visible in the upper left and lower right corners. The reason that the framing figures are only visible in a small area is that the frame is considerably curved. Similarly, canvas on the back side of the panel is only partially visible, see Fig. 4b. The effect of the panel's deformation on image visualisation can be resolved by a virtual flattening of the panel, as will be shown in the next chapter.

As already mentioned, it cannot be directly determined whether the value of the calculated CT density is due to the homogeneity of the material or its chemical composition. This problem can be solved to some extent by using DECT [11], as shown in Fig. 5. As already mentioned, the artwork was examined using two different acceleration voltages of 80 kV and 180 kV.

DECT is, in general, based on a linear combination of CT data taken at such different low and high-energy spectra. In our case, this was done by subtracting the volume reconstructed from projections obtained at the lower X-ray tube voltage (low-energy spectrum) from the reconstruction from the data recorded at the higher X-ray tube voltage (high-energy spectrum). This process description is formally written in the following equation:

$$\mathrm{Vol}_{\mathrm{DECT}} = \mathrm{Vol}_{180\mathrm{kV}} - \mathrm{wf} \bullet \mathrm{Vol}_{80\mathrm{kV}} \qquad (1)$$

The 80 kV data scaled by the wf weighting factor are subtracted from the 180 kV data. The choice of the weighting factor value depends on what we want to highlight. Here, it is set heuristically. In the case of relatively homogeneous materials, it can also be

Fig. 3 An example of the technology of connecting the components of a wooden panel. The contact surfaces of the parts were roughened before gluing (**a**). Several cracks are easily recognisable (**b**)
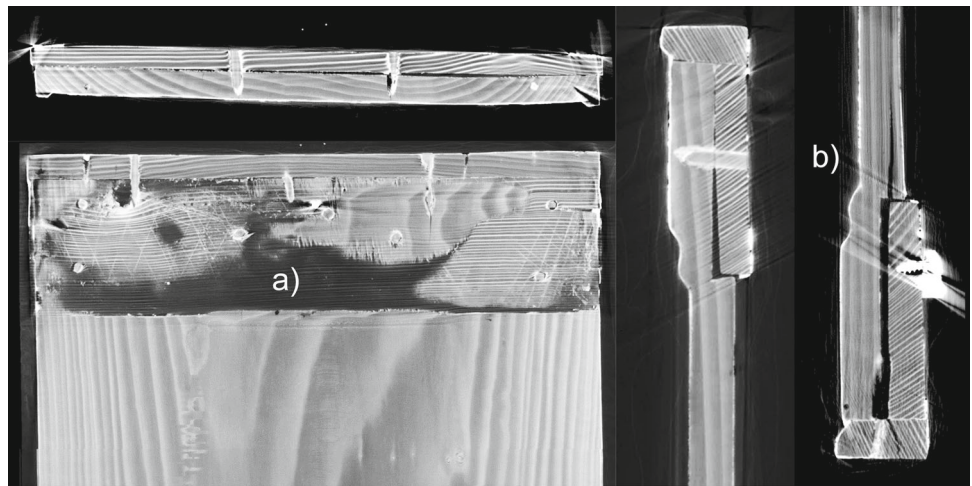

Fig. 4 A section passing through the panel near the front surface of the frame **a**, the figures are only partially visible. A section taken from the back **b**, the canvas is clearly discernible, although the surface to which it is applied is not flat
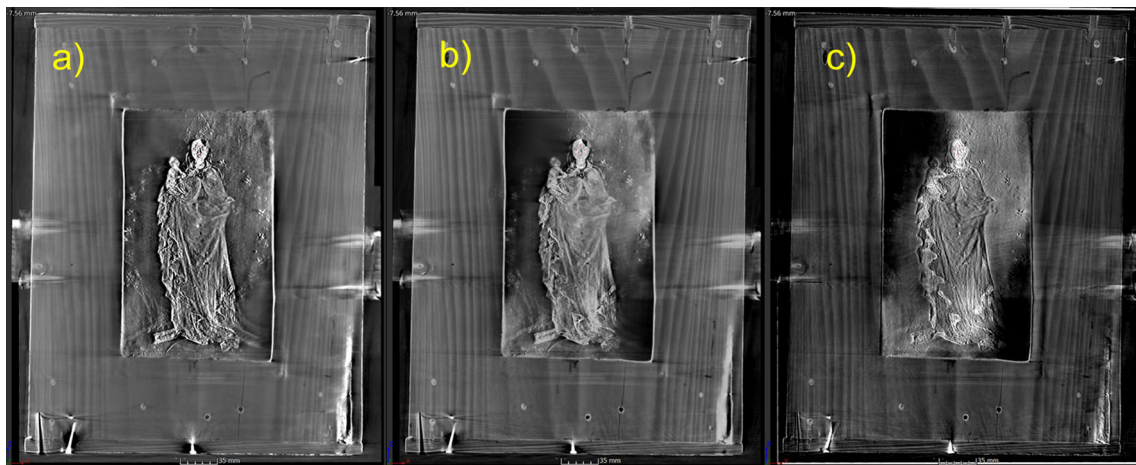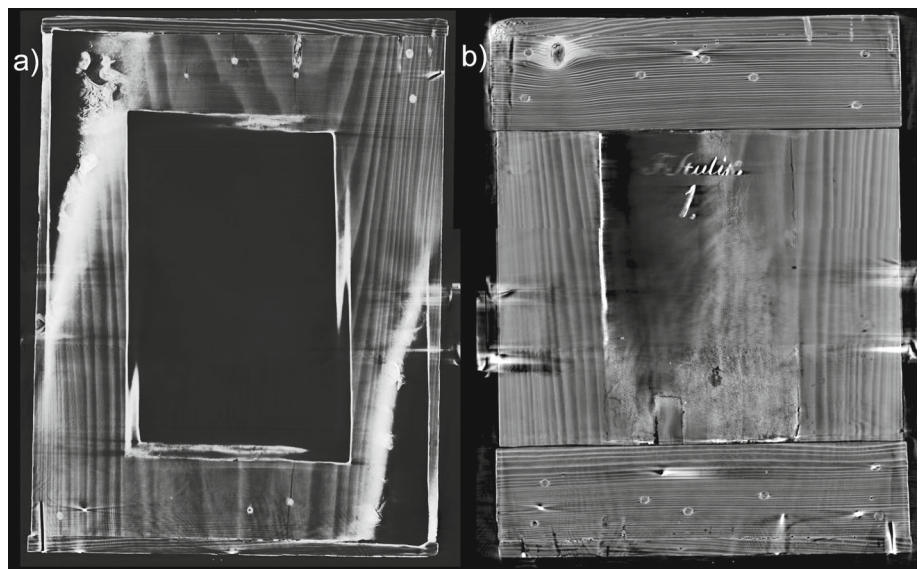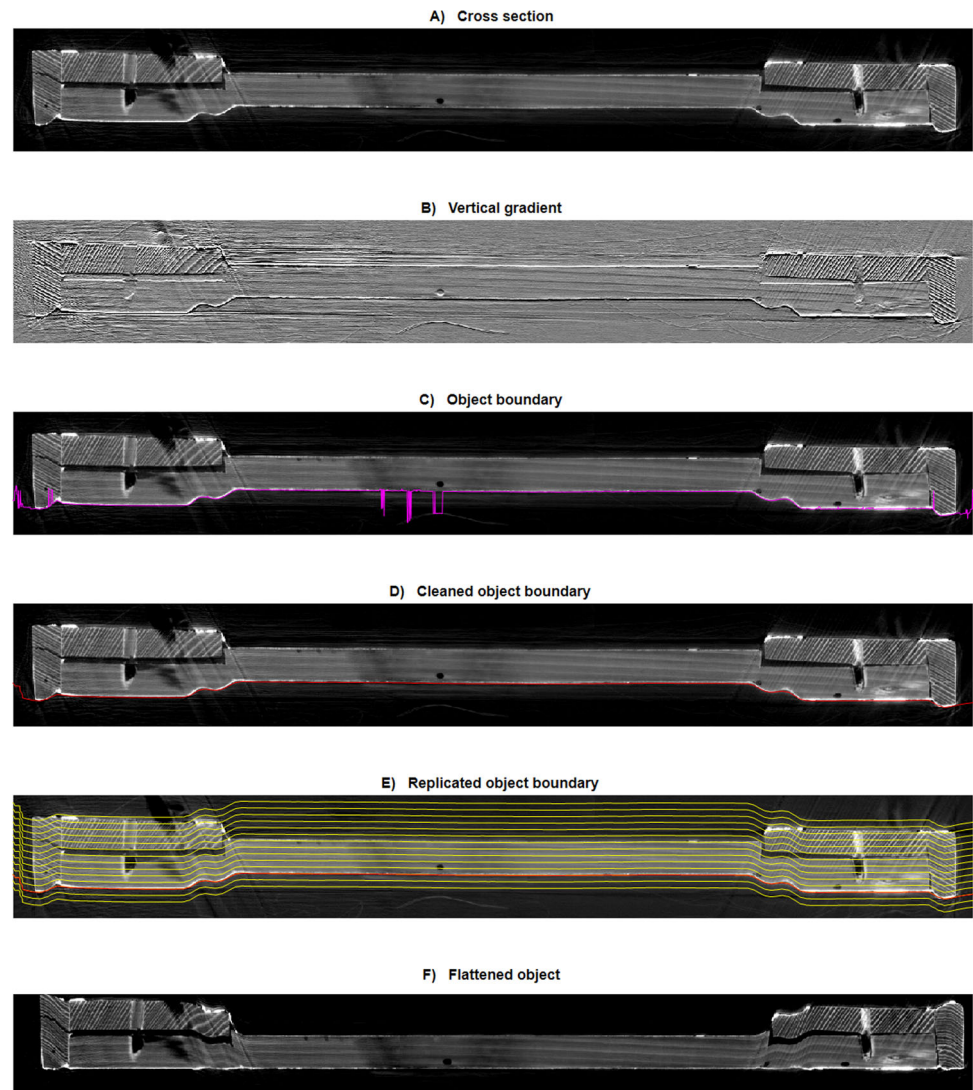

Fig. 5 CT reconstruction based on 80 kV projections **a** and on 180 kV projections **b** High attenuation materials (lead white and vermillion) are more resolvable in the DECT data **c**

calculated [11]. An example of such DECT data processing is shown in Fig. 5, where the wf value was set to 0.3 to highlight high *Z* elements.

Fig. 6 Visual depiction of the flattening procedure

4 Flattening of the tomographic volume

The virtual flattening of the tomographically created 3D virtual model is based on a transformation from a coordinate system defined by the general surface of the object under study to an orthogonal coordinate system. In the case of a panel image, both coordinate axes in the panel plane are standard orthogonal. Only the coordinate perpendicular to the panel plane has a general description defined by the shape of the outer surface of the panel on the side of interest. It is therefore necessary to obtain a description of the panel's front side, where the image is located.

Although the data is processed in 3D space, we will illustrate the flattening procedure in 2D for ease of explanation (Fig. 6). The steps used in the flattening procedure are described below.

(A)   Obtain a horizontal cross section (section) of the artwork. The front side of the panel is oriented downwards here and for all sub-figures.
(B)   Compute the gradient of the tomographic data density perpendicularly to the panel plane.
(C)   Find the boundary of the object, as defined by the maximum gradient. The contour is sometimes outside the object boundary, which is due to in homogeneities in the painting or because the gradient in the packaging material outside the object is higher.
(D)   Clean data from the previous step. First, an intensive smoothing filter is applied, points differing significantly from the smoothed data are interpolated, and the resulting data are smoothed with a less intensive filter. Note that the object boundary is searched for the entire painting area at once, not separately section by section. We will therefore continue to use the term boundary surface for the object boundary and refer to it as "b".

Fig. 7 Flattened panel panting from the obverse side (**a**); from the reverse side (**b**)—canvas is clearly visible as well as decorative frames made of vermilion

(E) Replicate the object boundary surface with an increment equal to the voxel size (in the corresponding image, here, only every 25 is plotted for clarity). The set of these boundary surfaces defines the coordinate system perpendicular to the image plane, hereafter referred as "*B*".

(F) Produce a flattened object. The entire object is straightened, so that it has a frontal face flat and parallel to the image plane.

The first four steps of the flattening procedure are quite standard and commonly available, for example in the already mentioned VGmax software. Nevertheless, the whole procedure described above was fully implemented in MATLAB software. The core of the procedure related to the last two points, (E) and (F) processed in 3D, can be written in MATLAB code as follows:for ii = 1: size(A,1)

B(ii,:,:) = b− mean(b) + ii + 1;end

[X,∼,Z] = meshgrid(1:size(B,2),1:size(B,1),1:size(B,3));flatA = interp3(A,X,B,Z);

Here, *A* is referring to the original object, and *flatA* is the flattened object. Variable *b* denotes the vertical coordinates of the identified object boundary, as mentioned in point D). Variable *B* is created by replicating the found boundary *b*, with a step equal to one, i.e. with the same resolution as the original object. (The resolution can be higher or lower, if necessary) The function *meshgrid* generates an orthogonal coordinate system, where the *X* and *Z* are defined by the volume size of *B*. The *interp3* function linearly interpolates the values of *A* to grid points defined by the three variables *X, B,* and *Z*. In our case, it is actually a one-dimensional problem, where each column of a particular section is shifted by the difference between the found boundary of object *b* and its mean value. However, this operation can be more complex, for example if the length of the object boundary is required to be preserved.

Let us note that the described procedure ensures that the context of the whole object is preserved, although its overall shape may be disturbed by straightening. In addition, if this procedure is applied to a panel where no profiled frame is present (only one smooth panel), the resulting panel becomes flat without distorting its internal structure. It has already been tested that the outside shape can be described by a suitable polynomial surface for such panels, instead of item D in the procedure description. This solution is particularly suitable for paintings containing pigments with low X-ray attenuation, where therefore finding the panel surface based on the gradient is not very reliable over the entire painting area and many boundary data need to be interpolated.

5 Virgin and child on a crescent moon survey based on flattened CT reconstruction

CT data of the Virgin and Child on a Crescent Moon recorded at 180 kV were flattened both from the front side (Fig. 7a), as well from the back side (Fig. 7b).

As the thickness of the individual layers of the painting is usually in the lower tens of micrometres, it is not possible to distinguish the individual layers of the painting using the presented CT methodology, as the result obtained was 83.7 μm perpendicularly to the panel plane. However, it is possible to distinguish the basic panel painting composition based on the flattening.

Figure 8a presents the surface of the wood being roughened to improve the adhesion for canvas gluing. The structure of the canvas covering the entire panel can be seen in Fig. 8b. The distribution of the chalk ground is shown in Fig. 9a. Note that its thickness is higher on the frame than in the central part of the painting. The top layer of the painting is depicted in Fig. 9b. Compared with

Fig. 8 Roughened panel surface **a**, the grooves in the area of the central motif are more pronounced than on the frame, weighting factor wf = 0.3 from Eq. (1); canvas texture **b** is + 0.32 mm above the wood panel face, wf = 0.5
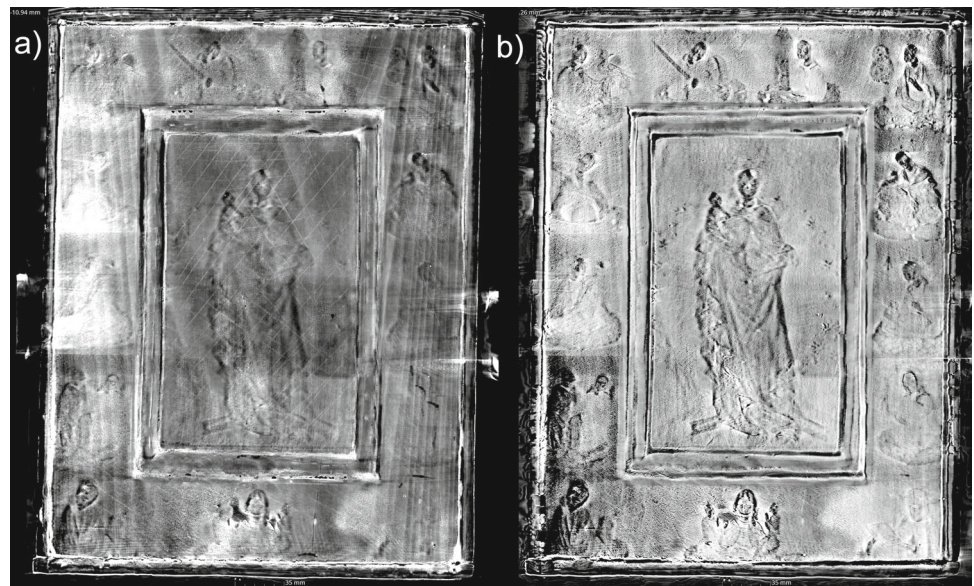

Fig. 9 Chalk ground distribution **a** is + 0.72 mm above the wood panel face (wf = 0.5); the painting itself **b** is + 0.88 mm above the face of the wooden panel (wf = 0.35) – Saint Barbara is marked with letter A, Saint Dorothy with B, Saint Agnes with C, Saint Ursula with D, Saint Genevieve with E and the cleric and Poor Clare with F
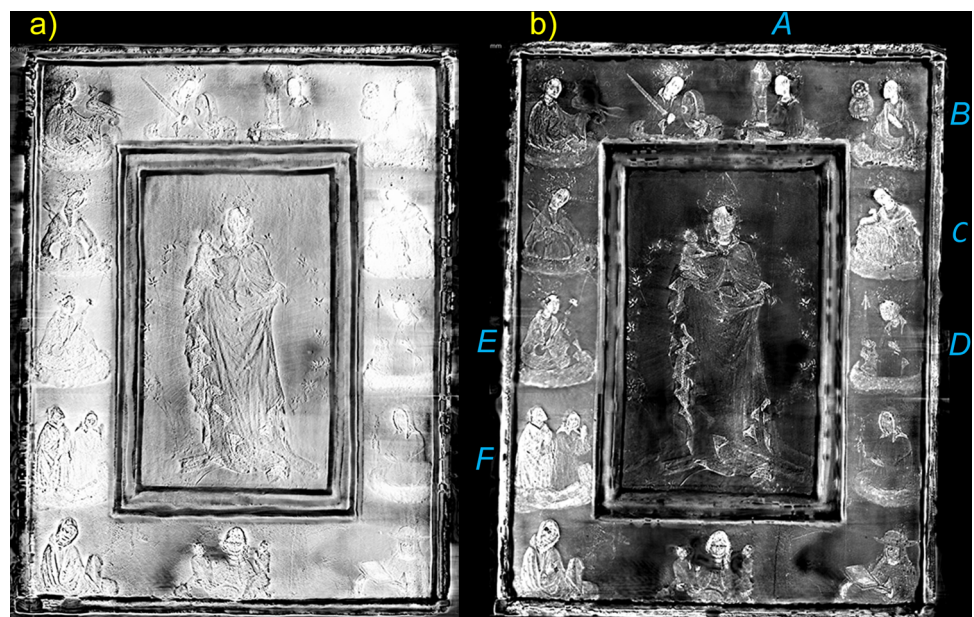
Fig. 7a, the chalk ground affecting the visibility of the figures on the frame is suppressed. It can be observed that even after virtual flattening, the resultant volumes are not perfectly flat, but the inaccuracies are only in the range of several voxels.

Figure 10 shows six figures from the frame, for which their section position has been slightly adapted to correspond to the individual figure(s). The same details, which are not fully apparent in the overall image (Fig. 9), become visible. For example, the black spots correspond to previous restorations, whilst the white lines that represent the engraved underpainting are clearly visible in St. Barbara's cloak, for instance (see *A* in Fig. 10). The decorations formed by punching are also visible. In addition, various discrepancies have been found between the calculated CT densities and the colours in visible light, for example for the red cloak of St. Agnes and St. Ursula, compare Figs. 1a and 10. This served as a motivation for further material analyses, see the following section.

6 Complementary XRF and Raman material analysis discussed with the CT survey

To expand our knowledge about the materials used, the CT survey was supplemented with photomicrographic documentation using a Dino-Lite Pro AM4113ZTFV2W USB microscope, featuring polarised visible and ultraviolet light ($\lambda = 375$ nm) and 1.3 megapixel, magnification $50 \times$, $200 \times$. The X-ray fluorescence analysis was performed using a portable NITON XL3t GOLDD
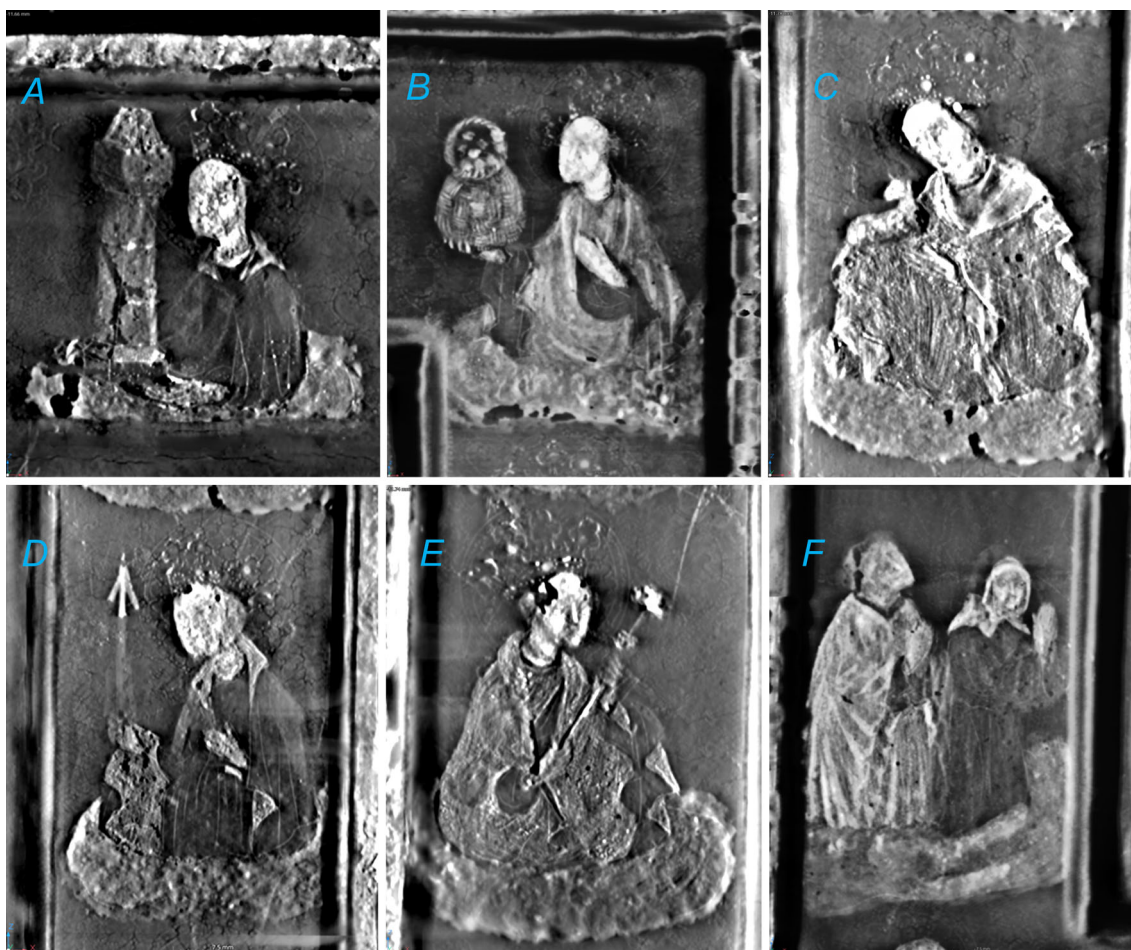
Fig. 10 Several framed figures in detail: top row – St. Barbara, St. Dorothy and St. Agnes; bottom row—St. Ursula, St. Genevieve, and the cleric and Poor Clare. The positions of the corresponding planes in which they lie have been chosen in order to make the structures as visible as possible; ~0.92 mm from the surface of the wood of the frame (wf = 0.35)
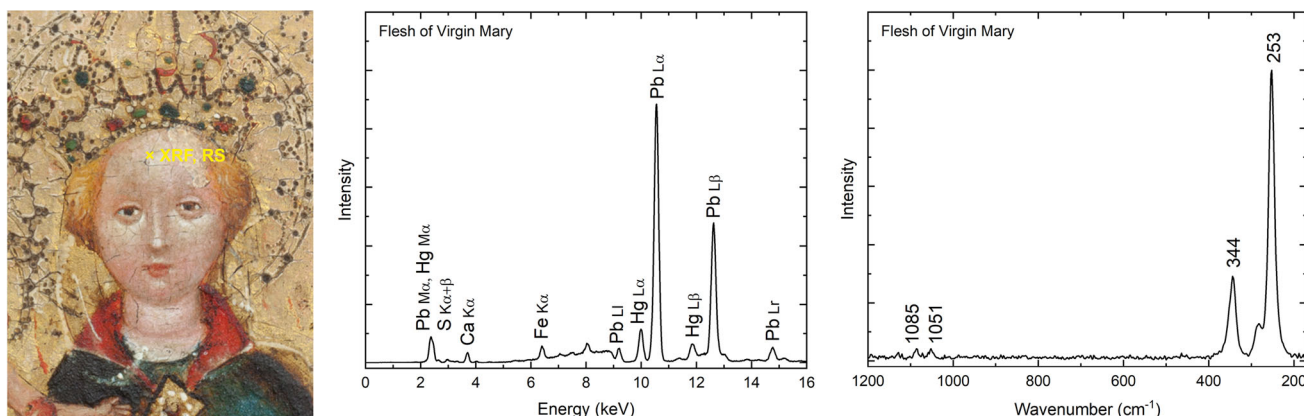

Fig. 11 Detail of the face of the Virgin Mary and XRF and Raman spectra of the flesh tone of Mary's cheek

instrument (Thermo Scientific, US) with a mini X-ray source equipped with a silver anode and allowing maximum accelerating voltage of 50 kV. Elements heavier than aluminium (Z > 13) were detected. An integrated silicon detector was used to determine the radiation emitted from the surface of the painting from an area with a minimum diameter of 3 mm. The measured area was photographed with an integrated CCD camera. Each analysis took cca 135 s. The measurements were taken without any direct contact with the painting from a distance 5 mm approximately. A Bravo spectrometer (Bruker, DE) was used for the mobile Raman spectroscopy. The instrument is equipped with a dual laser with suppressed fluorescence—Sequentially Shifted Excitation (SSE).

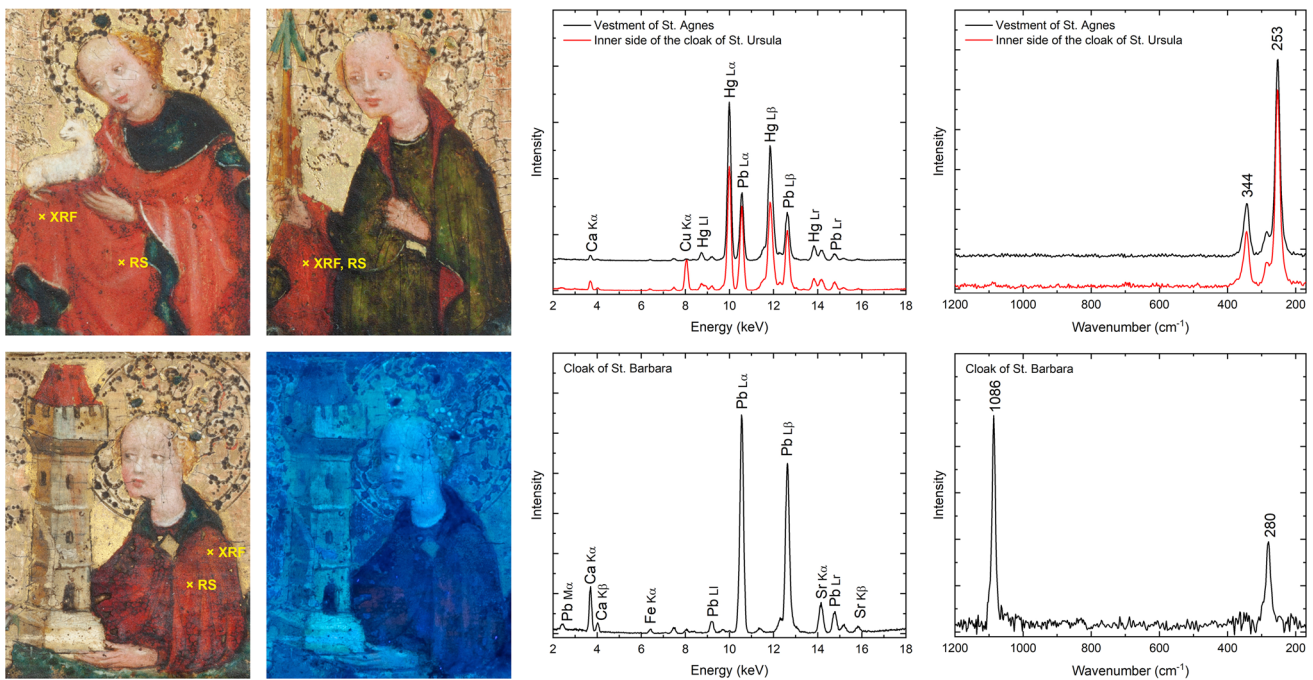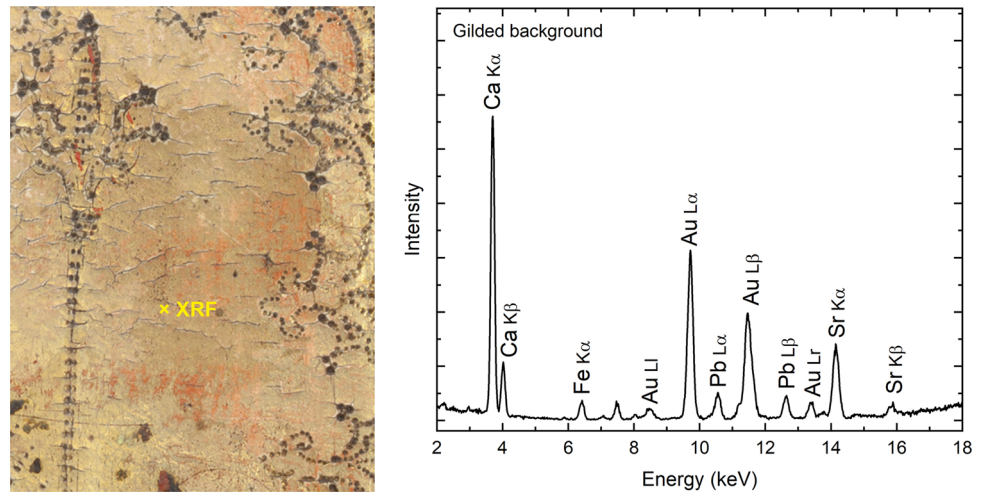**Fig. 12** Detail of the gilded background and corresponding XRF spectrum

Fig. 13 Details of St. Agnes and St. Ursula and XRF and Raman spectra of the red vestment and the inner side of the cloak (top row); detail of St. Barbara in visible and UV light and XRF and Raman spectrum of the red cloak (bottom row)

The measurements were taken in a spectral range of $170 - 3200$ cm^{-1} with a laser output < 100 mW and a spectral resolution of $10 - 12$ cm^{-1}. The measurements were taken from the surface of the painting. The evaluation was performed using the Opus programme. The spectra were compared with the spectral library of the Chemical-Technological Laboratory of the National Gallery Prague.

The grey levels in Fig. 9b correspond to the calculated CT density, which is affected by the composition and homogeneity of the layer. A lighter shade in the figure indicates a higher local density and vice versa. Dense layers containing high amounts of heavy elements, e.g. lead and mercury from lead white ($2\,PbCO_3 \cdot Pb(OH)_2$) and vermilion (HgS), respectively, are characterised by a light shade, which appears, for example, in the flesh tones (mainly faces and hands) of the figures in the top right corner of the CT section in Fig. 9b (St. Barbara, St. Dorothy and St. Agnes, labelled *A*, *B*, and *C* in Figs. 9b and 10). The flesh of the Virgin Mary in the central scene is darker, although the composition is similar to the flesh tones on the frame figures. Analysis of the material confirmed the presence of lead white (characteristic Raman band at ~ 1051 cm^{-1}) and vermilion (characteristic Raman bands at ~ 344 and 253 cm^{-1}) with an admixture of ochres (a mixture of aluminosilicates with Fe_2O_3 iron oxide, see Fig. 11). This is due to the fact that the paint layer of the Virgin's body is finer and that the resulting shade is more influenced by the surrounding layers, especially the chalk ground ($CaCO_3$, characteristic Raman bands at ~ 1085 and 280 cm^{-1}). The gilded background looks dark in CT section,

even though it contains gold, but the layer is too thin (usually about 2—3 µm) [12–14] and partially rubbed out (Fig. 12), so it has little effect on the resulting local CT density (voxels are larger than layer thicknesses).

A distinct light shade is also evident on the white cloak of the cleric (*F* in Fig. 10) made of lead white and on the red vestment of St. Agnes (*C* in Fig. 10), where elemental analysis showed high lead and mercury content. Raman spectroscopy confirmed the use of vermilion (Fig. 13). The lead probably comes from lead white, but red lead (Pb_3O_4) cannot be ruled out, although Raman spectroscopy did not prove its presence. Similar results of material analysis were obtained from the red cloak of St. Genevieve (*E* in Fig. 10) and the inner side of the cloak of St. Ursula (copper is present in the green paint of the outer side of the cloak, *D* in Fig. 10). The darker shade in the CT section is probably due to a thinner layer of paint rather than any difference in composition. Different pigments were identified on St. Barbara's cloak (*A* in Fig. 10), where red ochre and red lake were used instead of vermilion. Red lake pigment was identified based on its characteristic fluorescence after excitation with UV light. Calcium carbonate (chalk) and lead white were also identified. The presence of only small amounts of heavy elements resulted in a significantly darker hue compared to the other red areas.

Although it is not possible to distinguish the individual layers of paint, the CT scan clearly shows even minor shifts in the composition and thickness of the layers.

7 Conclusion

This survey allowed for a non-destructive evaluation of the current state of panel painting, including defects in its internal structure, and for furthering the knowledge of panel painting production technology. It provided data for dendrochronological dating and helped to identify areas of interest suitable for further analyses. The obtained results will be compared with the material research of the Lanna's Madonna (c. 1450, inv. No. O 494, 50.5×38.5 cm) in order to verify whether both works come from the same workshop, which is assumed on the basis of analyses of stylistic and painting techniques carried out by the art historian.

Data availability No Data associated in the manuscript.

References

1. J. Pešina, Česká malba pozdní gotiky a renesance (Prague), pp. 18–19, cat. No. 15 (1950)
2. J. Fajt, Š. Chlumská, Bohemia and Central Europe 1200–1550. The Permanent Exhibition of the Collection of Old Masters of the National Gallery in Prague at the Convent of St Agnes of Bohemia (The National Gallery in Prague, Prague, 2006), pp. 69, cat. No. 86, p. 145.
3. H. Dáňová, Š. Chlumská, R. Šefců (edd.), For the Eyes to Admire: Decorative Techniques in Medieval Painting and Sculpture, 14th-16th Centuries (The National Gallery in Prague, Prague, 2017), pp. 212–215 (bibliography).
4. T. Kyncl, in *In Depth and on the Surface* Š. Chlumská, R. Šefců, V. Antušková (eds.) The National Gallery in Prague, Prague, pp. 67–73 (2022)
5. Š. Chlumská, R. Šefců, V. Antušková (eds.), In Depth and on the Surface, The National Gallery in Prague, Prague, (2022).
6. F. Albertin et al., "Ecce Homo" by Antonello da Messina, From non-invasive investigations to data fusion and dissemination. Sci Rep **11**, 15868 (2021). https://doi.org/10.1038/s41598-021-95212-2
7. S. Legrand et al., Examination of historical paintings by state-of-the-art hyperspectral imaging methods: from scanning infra-red spectroscopy to computed X-ray laminography. Herit Sci **2**, 13 (2014). https://doi.org/10.1186/2050-7445-2-13
8. M. Dominguez-Delmás et al., X-ray computed tomography for non-invasive dendrochronology reveals a concealed double panelling on a painting from Rubens' studio. PLoS ONE **16**(8), e0255792 (2021). https://doi.org/10.1371/journal.pone.0255792
9. L. Montaina et al., Assessment of the panel support of a seventeenth-century dutch painting by clinical multislice computed tomography. Stud. Conserv. **66**(3), 174–181 (2021). https://doi.org/10.1080/00393630.2020.1757881
10. T. Fila et al., Utilization of dual-source X-ray tomography for reduction of scanning time of wooden samples. J. Instrum. **10**(05), C05008–C05008 (2015). https://doi.org/10.1088/1748-0221/10/05/C05008
11. D. Vavrik et al., Dual energy CT inspection of a carbon fibre reinforced plastic composite combined with metal components. Nondestructive Testing and Evaluation **6**, 47–55 (2016). https://doi.org/10.1016/j.csndt.2016.05.001
12. P. Mactaggart, Practical Gilding. London (2002).
13. K. von Baum, et al. Let the Material Talk: Technology of Late-medieval Cologne Panel Painting London (2014).
14. R. Šefců, Gold, Silver and Zwischgold, in *For the Eyes to Admire: Decorative Techniques In Painting and Sculpture, 14th–16th Century*. ed. by H. Dáňová, Š. Chlumská, R. Šefců (The National Gallery in Prague, 2017), pp.8–29